

Light intensity dependence of photocurrent gain in single-crystal diamond detectors

Meiyong Liao,* Xi Wang,† Tokuyuku Teraji, Satoshi Koizumi, and Yasuo Koide

Sensor Materials Center, National Institute for Materials Science (NIMS), 1-1 Namiki, Tsukuba, Ibaraki 305-0044, Japan

(Received 4 August 2009; revised manuscript received 26 November 2009; published 13 January 2010)

The authors report on the photocurrent gain in a diamond photodetector that has two nonohmic contacts connected back-to-back. This photocurrent gain strongly depends on both the deep-ultraviolet (DUV) light intensity and the applied voltage. In addition, the gain is accompanied by a slow response. The gain is observed to originate from a metal/diamond interface trap center. Numerical analysis discloses that the photocurrent-voltage characteristics follow thermionic-field emission tunneling at low DUV light intensity and field-emission tunneling at high DUV light intensity. The deep traps are thought to produce a thin interface barrier layer at the metal/diamond interface under DUV illumination, which is responsible for the tunneling processes.

DOI: [10.1103/PhysRevB.81.033304](https://doi.org/10.1103/PhysRevB.81.033304)

PACS number(s): 72.40.+w, 73.40.Sx, 85.60.Dw

The interest in the utilization of diamond for deep-ultraviolet (DUV) detection has been triggered due to its extreme properties and the progress in the development of high-quality single-crystal diamond layers.¹⁻⁵ An important issue for practical devices is to achieve high responsivity or photocurrent gain while maintaining a fast response time. The high responsivity is important for weak signal detection such as flame or chemical sensing and DUV imaging with reduced pixel size.

One strategy to generate photocurrent gain is to utilize quantum well structures or to introduce deep bulk defects.^{6,7} As for diamond photodetectors, the incorporation of boron in the homoepitaxial layer can greatly improve the responsivity. In that case, the boron in the epilayer and the nitrogen in the substrate were dominant factors in the photoresponse behavior due to the formation of a *p-n* junction at the interface. A huge photocurrent gain was obtained when the boron content in the epilayer was relatively high, which was explained in terms of deeply trapped carriers by the ionized nitrogen in the substrate.⁷ Since such a gain mechanism is controlled by the carrier transport in the epilayer, the metal contact to the diamond layer must be the ohmic type or Schottky type in the forward bias mode. In fact, no photocurrent gain was observed in the devices in our previous work if the metal/diamond contacts were the blocking type.⁸ In this work, we report that photocurrent gain can be generated as the DUV light intensity increases in a homoepitaxial diamond photodetector with two nonohmic contacts connected back-to-back. The transient photocurrent behavior at different biases and the temperature effect on the photocurrent gain are investigated to understand the gain mechanism.

The diamond layer was grown on a high-pressure high-temperature type-Ib (100) substrate using a microwave plasma-enhanced chemical vapor deposition reactor, which makes it possible to deposit a diamond epilayer at a much higher speed than our previous system. Hydrogen and methane gases were fed for diamond growth. In this apparatus, a higher methane concentration with a CH₄/H₂ flow ratio of 2% was applied to achieve a higher growth rate. The substrate was heated to 1000–1090 °C by high power plasma during growth. The total pressure of the chamber during growth was maintained at 80 Torr. Since this growth system has never been used for boron doping, the resulting diamond epilayer is believed to be boron free. The homoepitaxial layer surface was oxidized in a common boiling acid solu-

tion. Interdigitated metal-semiconductor-metal (MSM) devices were fabricated using a standard photolithography process. The finger width and spacing were both 10 μm, and the optical receiving area was 5.2 × 10⁻² mm². A tungsten carbide film with a thickness of 10 nm was deposited as the electrical contact.⁸

The current-voltage (I-V) characteristics were measured using a two-point probe method with an Advantest picoammeter (R8340A) and a dc voltage source (R6144). A dc current mode was employed to record the spectral response, in which a 500-W Ushio xenon lamp and an Acton research monochromator with order sorting filters were used. The light intensity was modulated through an aperture and calibrated by using a UV-enhanced Si photodiode.

The dark current of the device was below the detection limit of the measurement system (<10⁻¹³ A) for the biases examined. Figure 1(a) shows the I-V characteristics of the MSM device upon illuminating the 220 nm light with different light intensities. Two different I-V regions are observed. At low biases, the I-V characteristics exhibit sublinear behavior. At the bias larger than a critical value, e.g., 16 V at 1.3 μW/cm², the photocurrent increases superlinearly. The basic shapes of the I-V curves are similar to each other at various DUV intensities. However, the critical voltage, at which the second region appears, shifts to the lower side as the DUV intensity increases. In Fig. 1(b) the dependence of the photocurrent gain (the quantum efficiency is assumed to be unity) on the applied voltage at different DUV intensities is displayed. It is observed that the gain depends on both the incident light intensity and the applied bias. Figure 2 plots the gain as a function of the incident light intensities at a bias of 5 V in the sublinear region and 32 V in the superlinear region, shown in Fig. 1. In the sublinear region at 5 V, the gain is smaller than unity and independent of the light intensity. In the superlinear region at 32 V, the gain increases from unity to around 6 when the DUV intensity increases from 4.8 to 20 μW/cm².

It is interesting to note that the transient behavior of the photocurrent also depends on both the applied bias and the DUV intensity, as shown in Fig. 3. The response is fast at low biases or in the sublinear I-V region in Fig. 1, where the gain is smaller than unity, while it becomes slow at high biases or in the superlinear I-V region. The critical voltage, at which slow response occurs, shifts to lower values as the DUV intensity increases [Fig. 3(b)]. The transient response

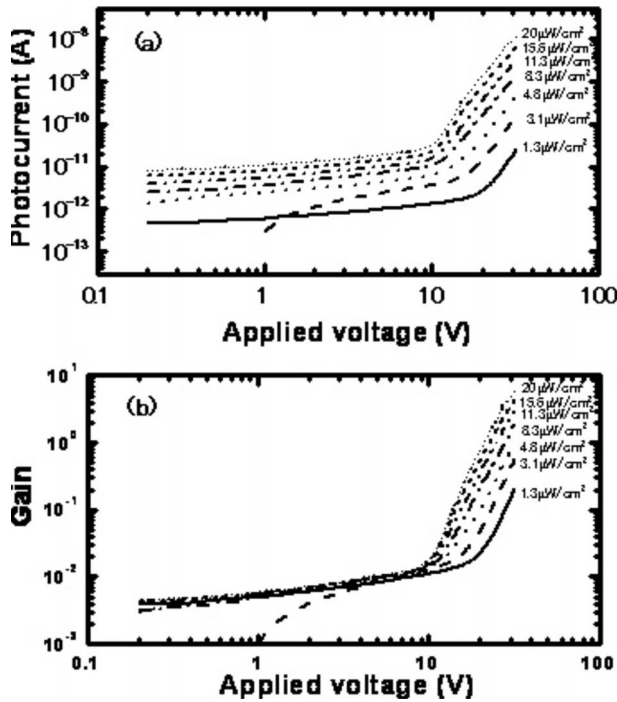


FIG. 1. (a) Photocurrent-voltage dependence at various DUV light intensities and (b) photocurrent gain-voltage characteristics at different DUV intensities. Two regions can be seen.

reveals that the photocurrent gain is accompanied by a relatively slow response at a high bias of 32 V. Therefore, the photocurrent gain is associated with some trapping events of photogenerated carriers.⁹

To further investigate the trap-related photocurrent behavior, we measured the photocurrent-voltage characteristics by illuminating DUV light with different intensities at elevated temperatures. The dependence of the photocurrent on the measurement temperature is illustrated in Fig. 4 for a similar MSM device, in which the applied biases are 5 and 32 V, and the DUV light intensity is $16 \mu\text{W}/\text{cm}^2$. As can be seen, at the bias of 5 V, the photocurrent does not vary with the temperature. In contrast, at 32 V, the photocurrent first experiences an increase as the temperature increases to 65°C , after which the photocurrent decreases monotonically with the temperature. From the Arrhenius plots of the photocurrent dependence on temperature at 32 V, a thermal activation

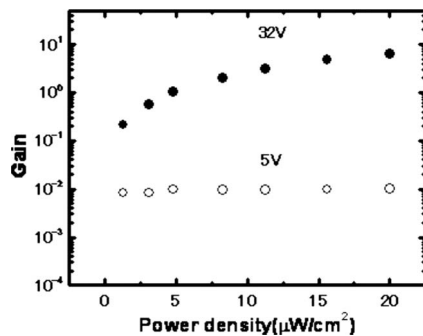


FIG. 2. The dependence of photocurrent gains on DUV light intensity at 5 V in the sublinear region and 32 V in the superlinear region.

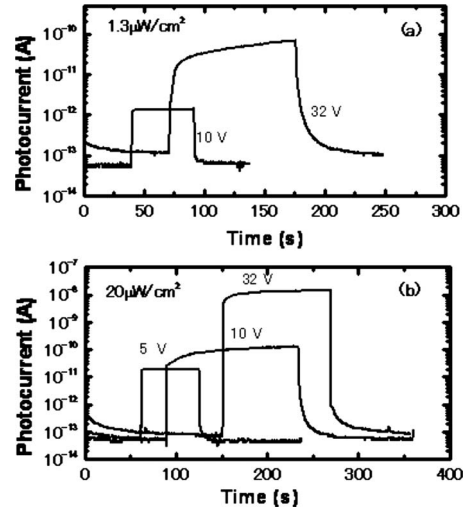


FIG. 3. Transient response upon DUV light at different intensities for various applied voltages. (a) $1.3 \mu\text{W}/\text{cm}^2$ and (b) $20 \mu\text{W}/\text{cm}^2$.

energy around 0.2 eV was obtained. The independence of the photocurrent on the temperature at 5 V excludes the bulk defects as a primary reason for the gain. The decrease in the photocurrent at 32 V suggests that some of the trapped carriers relax at high temperatures.¹⁰ Similar temperature-dependent behavior was also observed for a weaker DUV intensity ($1.3 \mu\text{W}/\text{cm}^2$). It should be noted that no dark current was observed as the measurement temperature increased.

Previously, the photocurrent gain was reported when the contacts of the MSM devices were annealed or a Schottky photodiode was operated in the forward bias mode.^{8,11} In both cases, the ohmic contact was a prerequisite because charge injection led to the gain. In the present study, no post-annealing treatment was applied. Therefore, in this back-to-back MSM device configuration, the WC/diamond

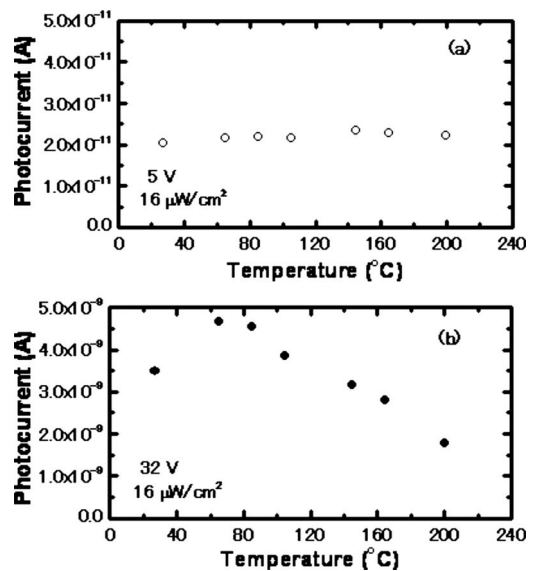


FIG. 4. Dependence of photocurrent on measurement temperature at a DUV intensity of $16 \mu\text{W}/\text{cm}^2$ at the biases of (a) 5 V and (b) 32 V.

interface is basically blocking for carrier transport in dark. Alternative mechanisms rather than ohmic-type charge injection are assumed to be responsible for the photocurrent gain. An impact ionization mechanism due to field enhancement in the electrode edge was suggested as the reason for the photocurrent gain at high applied biases.¹¹ This field enhancement, however, is difficult to explain the increase in the photocurrent at the temperature from RT to 65 °C, since the impact ionization will be suppressed monotonically due to phonon scattering at elevated temperatures.¹²

Considering the facts that (i) a gain larger than unity appears at high biases (i.e., 32 V) and is accompanied by a slow time response, (ii) the gain decreases when the measurement temperature is above 105 °C at high biases (i.e., 32 V), and (iii) the photocurrent shows no dependence on the DUV intensity or the measurement temperature at low biases (i.e., 5 V), we propose that the gain larger than unity is related to charge trapping at the metal/diamond interface during DUV illumination. No dark conductivity at elevated temperatures suggests that the interface defect acts as an acceptor during DUV illumination. This acceptor leads to the bending of the interface band and the formation of a thin interface barrier layer between the metal and diamond. This thin interface barrier layer thus leads to hole tunneling from the metal to the diamond layer above a certain bias, which contributes to the gain. Thermionic-field emission (TFE) or field emission (FE) of majority carriers through the metal/diamond interface barrier is put forward here as the reason for the photocurrent gain at high applied biases. The thermionic-field emission current through a thin interface barrier can be expressed as¹³

$$J_{\text{TFE}} = J_s \exp\left(\frac{q(V + V_p)}{\varepsilon'}\right), \quad (1)$$

where

$$J_s = \frac{A^* T (\pi q E_{00})^{1/2}}{k} \exp\left(-\frac{q(\phi_B - V_p)}{E_0}\right) \left[V - V_p + \frac{\phi_B}{\cosh^2(E_{00}/kT)} \right]^{1/2}, \quad (2)$$

$$\varepsilon' = \frac{E_{00}}{E_{00}/kT - \tanh(E_{00}/kT)}, \quad (3)$$

$$E_0 = E_{00} \coth(E_{00}/kT), \quad (4)$$

$$E_{00} = \frac{qh}{4\pi} \sqrt{\frac{N_t}{m^* \varepsilon_s}}, \quad (5)$$

$$V_p = \frac{kT}{q} \log\left(\frac{N_v}{p}\right). \quad (6)$$

Here, A^* is the Richard constant (96 A/cm²·K²), q is the electron charge, h is Planck's constant, k is the Boltzmann constant, m^* is the effective hole mass, ϕ_B is the Schottky barrier height of the WC/*p*-diamond interface, V is the applied bias, ε_s is the dielectric constant of diamond, p is the

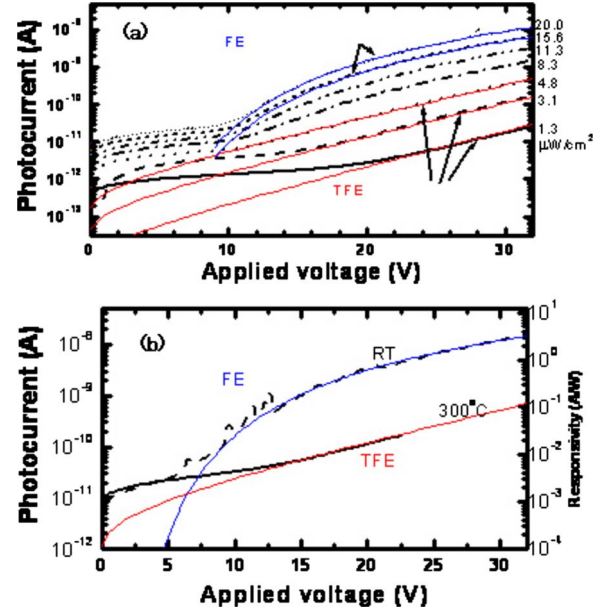


FIG. 5. (Color online) (a) Fitting of photocurrent vs. applied voltage curves by TFE and FE tunneling mechanisms and (b) fitting of the photocurrent vs applied voltage curves by FE mechanism at RT and TFE at 300 °C for DUV intensity larger than 5 $\mu\text{W}/\text{cm}^2$.

hole density in the illuminated region, V_p is the Fermi-level potential in the diamond, and N_v is the effective density of states in the valence band. E_{00} reflects the tunneling probability. Here, we assume that the deep trap with a concentration of N_t near the WC/diamond interface behaves as an acceptor. The field-emission tunneling current can be expressed by a Fowler-Nordheim process as¹⁴

$$J_{\text{FN}} \propto V^2 \exp\left(\frac{b}{V + a}\right), \quad (7)$$

where a and b are constants. These two injection mechanisms in Eqs. (1) and (7) were utilized to fit the I-V characteristics in Fig. 1. The fitting results are shown in Fig. 5(a), where $\Phi_B = 1.6$ V, $m^* = 0.8m_0$, and $\varepsilon_s = 5.7$ were used. For the J_{TFE} current fitting, the hole density was $2.1 \times 10^{17} \text{ cm}^{-3}$, and for the J_{FN} current fitting, a and b were -23.9 and -61.4 , respectively, for DUV intensity $P = 15.6 \mu\text{W}/\text{cm}^2$, and -23.3 and -60.4 , respectively, for $P = 20 \mu\text{W}/\text{cm}^2$. It was found that thermionic-field emission dominates the carrier transport at the metal/diamond interface when the DUV light power P is lower than around $5 \mu\text{W}/\text{cm}^2$. When P is larger than $15 \mu\text{W}/\text{cm}^2$, Fowler-Nordheim tunneling governs the photocurrent at the applied biases larger than 9 V. The fittings also reveal that the DUV illumination generates additional charge of acceptor-type traps close to the interface, which is the origin of the thin interface barrier. The trap density N_t is found by fitting to increase from $1.26 \times 10^{19} \text{ cm}^{-3}$ to $7.9 \times 10^{19} \text{ cm}^{-3}$ as the DUV intensity increases. Experimentally, it was also observed that there existed one unknown acceptorlike trap at the metal/diamond interface with a density of 10^{19} cm^{-3} .¹⁵

It was difficult to fit the photocurrent-voltage curves at different DUV intensities by using different hole densities.

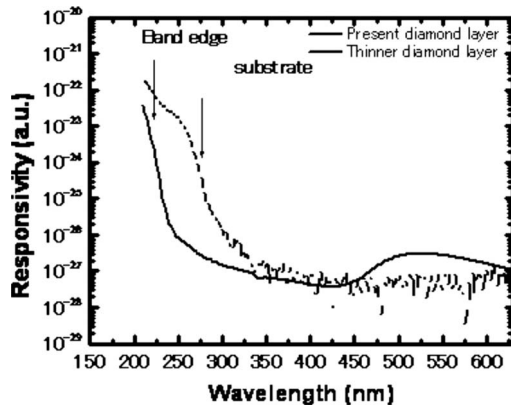


FIG. 6. Spectral response of the present MSM device with that of previous one on a thinner diamond layer (Ref. 16).

This may be because the free-electron-hole pair density (i.e., perfect crystal) directly generated by the DUV light is much smaller than that of the hole density induced by trapping behavior. Therefore, the interface traps have two roles: narrowing the metal/diamond barrier width and increasing the hole density.⁷

The temperature-dependent photocurrent-voltage characteristics at the DUV intensities larger than $5 \mu\text{W}/\text{cm}^2$ were also fitted, as shown in Fig. 5(b). The electrical transport mechanism was found to change from FE at RT to TFE at 300°C . This is because the traps are relaxed at 300°C , leading to a larger depletion width at the metal/diamond interface. The temperature-dependent photocurrent further suggests that the interface traps dominate the photocurrent transport mechanism.

The bias and DUV light intensity-dependent transient response can be well understood by the formation of a thin interface barrier induced by the traps mentioned above. At low applied biases or in the sublinear region, the applied field is insufficient to cause tunneling through the metal/diamond interface. Thus, the device behaves like a back-to-back Schottky photodiode with fast response, in which the carriers recombine at the electrodes. This can be revealed by the small constant photoresponsivity in the sublinear region. As the bias increases, thermionic-field emission or field-emission tunneling governs the photocurrent. Since the tunneling is due to charge traps, the gain is followed by a slow

time response. On the other hand, the metal/diamond interface barrier becomes narrower due to higher interface trap density as the DUV intensity increases, enhancing the tunneling probability. Therefore, the photocurrent gain is larger at a higher DUV intensity. Correspondingly, the bias for the gain decreases as the DUV intensity increases.

In the previous work, photocurrent gain was explained by bulk effects (boron and nitrogen incorporation). In that case, substrate nitrogen played a key role in the gain.⁷ To investigate the effect of the substrate nitrogen on the photocurrent gain, we measured the spectral response of the device by comparing it with that of previous reports.^{8,16} Figure 6 depicts the photoresponse spectra measured at 15 V, which were normalized by the incident photon flux. The overall shape of the spectral response does not depend on the applied bias. A distinct difference in the present device from the previous one is the disappearance of the dominant response at around 270 nm from the type-Ib diamond substrate.¹⁶ Instead, the sharp band-edge response is clearly seen. This feature suggests that the nitrogen in the substrate plays a weak role in the photoresponse here, due to the utilization of a thick intrinsic film. The spectral response excludes the substrate nitrogen as the main factor in the gain. On the other hand, it is clear that absorption occurs at around 500 nm. This absorption cannot be quenched by visible light as happened previously. It may form a deep defect within the homoepitaxial layer. This deep bulk defect, which interacts with the traps at the metal/diamond interface, may also contribute to the superlinear dependence of the gain on the DUV light intensity.⁹

In summary, photocurrent gain was observed in a homoepitaxial diamond photodetector with two nonohmic contacts connected back-to-back. The gain depended on either the DUV intensity or the applied biases. The DUV light illumination produced a thin interface barrier layer at the metal/diamond interface due to the existence of interface traps. Thermionic-field emission and field-emission tunneling were utilized to explain the photocurrent gain at low and high DUV intensity, respectively.

This work was partially supported by a Grant-in-Aid for Scientific Research from the Japanese Ministry of Education, Culture, Sports, Science and Technology (Grant No. 188517).

*meiyong.liao@nims.go.jp

†Present address: Department of Materials Science, Imperial College London, United Kingdom.

¹P. Bergonzo and R. B. Jackman, *Thin-Film Diamond II, Semiconductors and Semimetals 77*, edited by C. E. Nebel and J. Ristein (Elsevier, Amsterdam, 2004), Vol. 77, p. 197.

²A. De Sio *et al.*, Nucl. Instrum. Methods Phys. Res. A **583**, 125 (2007).

³M. Nesladek, Semicond. Sci. Technol. **20**, R19 (2005).

⁴A. BenMoussa *et al.*, Semicond. Sci. Technol. **23**, 035026 (2008).

⁵T. Teraji, Phys. Status Solidi A **203**, 3324 (2006).

⁶B. Movagharet *et al.*, Phys. Rev. B **78**, 115320 (2008).

⁷M. Liao *et al.*, Phys. Rev. B **78**, 045112 (2008).

⁸M. Y. Liao *et al.*, Appl. Phys. Lett. **90**, 123507 (2007).

⁹R. H. Bube, *Photoelectronic Properties of Semiconductors* (Cambridge, New York, 1992).

¹⁰M. Marinelli *et al.*, Appl. Phys. Lett. **83**, 3707 (2003).

¹¹Y. Iwakaji *et al.*, Appl. Surf. Sci. **254**, 6277 (2008).

¹²C. Groves *et al.*, IEEE Trans. Electron Devices **50**, 2027 (2003).

¹³H. Hasegawa and S. Oyama, J. Vac. Sci. Technol. B **20**, 1647 (2002).

¹⁴S. M. Sze, *Physics of Semiconductor Devices*, 2nd ed. (Wiley, New York, 1981).

¹⁵P. Muret *et al.*, Appl. Phys. Express **1**, 035003 (2008).

¹⁶M. Y. Liao *et al.*, Appl. Phys. Lett. **89**, 113509 (2006).